JOURNAL OF MATERIALS SCIENCE 25 (1990) 4933–4942

A review of particulate reinforcement theories for polymer composites

S. AHMED, F. R. JONES
School of Materials, University of Sheffield, Northumberland Road, Sheffield S10 2TZ, UK

A concerted survey is presented of the existing theories for predicting the strength and modulus of particulate-filled polymeric composites. The macroscopic behaviour of particulate composites is affected by the size, shape, and the distribution of the inclusions. The interfacial adhesion between the matrix and inclusion is also important. The limitation of theoretical models in describing these parameters and expressing the experimental data on the macroscopic behaviour is demonstrated.

1. Introduction

This review has been prompted by a renewed interest in the engineering application of particulate-filled materials. Addition of rigid particles to polymers or other matrices can produce a number of desirable effects; for example an increase in stiffness, a reduction in the coefficient of thermal expansion and an improvement in creep resistance and fracture toughness. The modulus of a filled resin results from a complex interplay between the properties of the individual constituent phases; the resin, the filler and the interfacial region. It is evident that the mechanical properties of the composite are affected by a number of parameters; the size, shape, aspect ratio and distribution of the reinforcing particles. In the case of non-spherical particles, the degree of orientation with respect to the applied stress is also important. This review will discuss how these parameters affect the experimentally observed macroscopic mechanical behaviour of particulate-filled polymers.

In the scientific literature a number of theories and equations have been developed to describe these phenomena but we have chosen to select for discussion those which best represent the experimental data. The limitation of these theoretical models will also be considered.

2. Modulus of particulate composites

The reinforcing effect of particles in polymeric materials was first recognized for rubber compounds. This arose from the development of an understanding of structure property relationship for carbon black-filled natural rubber. The viscous component of the viscoelastic properties, meant that the enhancement in modulus was considered to be analogous to increases in viscosity.

2.1. The theory of rigid inclusions in a non-rigid matrix

2.1.1. The Einstein equation

One of the earliest theories for a composite system was developed for elastomers and is based on Einstein's equation for the viscosity of a suspension of rigid spherical inclusions [1]

$$\eta_c = \eta_m(1 + K_E V_p) \quad (1)$$

where η_c and η_m are the viscosity of suspension and the matrix, respectively. K_E is the Einstein coefficient which is equal to 2.5, for spheres. V_p is the volume fraction of particulate inclusions. It has been assumed [2–4] that Equation 1 also holds for changes in the modulus (i.e., $\eta_c/\eta_m = G_c/G_m$), so that Equation 1 for shear modulus can be written

$$G_c = G_m(1 + 2.5V_p) \quad (2)$$

G is the shear modulus and p, m and c refer to particle, matrix and composite, respectively, throughout. For Einstein's equation (Equation 2), the stiffening action of a filler is independent of its size. The equation also implies that it is the volume occupied by the filler, not its weight, which is the important variable. This equation has only proved useful for low concentrations of filler because on increasing the volume fraction of filler the flow or strain fields around particles interact. The difficulties associated with defining these interactions lead to several modifications of Equation 2. The best is due to Mooney [5]. Equation 3 agrees with Einstein's equation at low volume fractions and represents the experimental data at higher volume fractions, the equation can be put into the form

$$G_c = G_m \exp\left(\frac{2.5V_p}{1 - SV_p}\right) \quad (3)$$

where S is the crowding factor (volume occupied by the filler/true volume of the filler). For close packed spheres $S = 1.35$. For non-spherical particles, the Mooney equation was subsequently modified according to Brodnyan [6]

$$G_c = G_m \exp\left(\frac{2.5V_p + 0.407(p - 1)^{1.508}V_p}{1 - SV_p}\right) \quad (4)$$

where p is the aspect ratio of the particle $1 < p < 15$.

Guth [7] generalized the Einstein concept by introducing a particle interaction term and showed that Equation 2 could be written in the form

$$G_c = G_m(1 + K_E V_p + 14.1V_p^2) \quad (5)$$

0022–2461/90 $03.00 + .12

He further assumed that the change in the elastic constant of the rubber by embedded spheres is entirely analogous to the theory of viscosity. When a rubber–carbon black suspension is stretched, the suspended particles perturb the stresses and strains set up in the body. This gives rise to an increase in elastic energy and therefore an increase in elastic constant. For spherical particles Equation 5 can be analogously written for E as

$$E_c = E_m(1 + K_E V_p + 14.1V_p^2) \quad (6)$$

For non-spherical particles he obtained

$$E_c = E_m(1 + 0.67pV_p + 1.62p^2V_p^2) \quad (7)$$

assuming $p \gg 1$.

For non-spherical particles, the shape factor, p was defined as the ratio of particle length to width. Other attempts at predicting E_c have been largely empirical using variable constants to fit the theoretical curve to the experimental data.

2.1.2. The Kerner equation

One of the most versatile and elaborate equations for a composite material consisting of spherical particles in a matrix, is due to Kerner [8]. For $G_p > G_m$, the Kerner equation simplifies to

$$G_c = G_m\left(1 + \frac{V_p}{V_m}\frac{15(1 - \nu_m)}{(8 - 10\nu_m)}\right) \quad (8)$$

where ν_m is the Poisson ratio of the matrix.

The equation has been modified [9–12] and the general form is given by Nielsen [12]

$$M = M_m\frac{1 + ABV_p}{1 - B\delta V_p} \quad (9)$$

where function $B\delta$ is dependent upon the particle packing fraction and M the modulus which may be for shear, elastic or bulk. The constant A accounts for factors such as the geometry of the filler and the Poisson ratio of the matrix. B accounts for the relative moduli of filler and the matrix phases.

In general, it is assumed that changes in relative viscosity with filler content will parallel the increase in modulus [2–4, 7]. Equation 3 is rewritten for elastic modulus and compared with the Kerner equation for $\nu_m = 0.39$ and $S = 1.35$ in Fig. 1. The Mooney equation predicts considerably more reinforcing action than the Kerner equation, and a modulus that tends to infinity at high volume fraction of filler. The equation assumes that $\nu_m = 0.5$ and that the modulus of the filler is infinitely greater than the matrix, both of which are not correct for a rigid matrix thus restricting the applicability of such models to filled rigid thermosetting polymeric matrices.

2.2. The theory of rigid inclusions in a rigid matrix

The random distribution of the constituent phases in a filled system demands a statistical approach, but this requires a knowledge of the distribution of the individual phases. Consequently, the problem has been simplified to a two-phase model in which average stresses and strains are considered to exist in each of the phases. The average behaviour of the composite is defined in terms of a representative volume element. When subjected to a gross uniform stress or strain, a uniform strain field is induced in the composite which can be used to estimate the elastic constant [4, 13, 14]. The other approaches consist of the establishment of bounds for the moduli by use of energy criteria in elasticity theory [15].

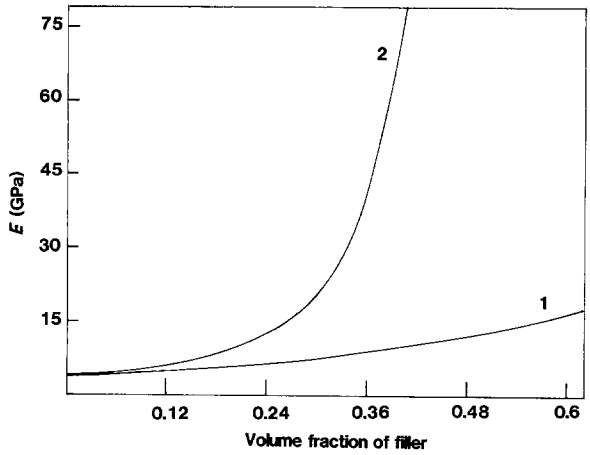

Figure 1 Theoretical predictions for the modulus of a particulate composite as a function of volume fraction. Curve 1 shows the Kerner equation $\nu_m = 0.39$ and curve 2 shows the Mooney equation for $S = 1.35$. Both curves were plotted with $E_m = 3.9$ GPa.

2.2.1. The series and parallel models

In the simplest possible case for a two-phase material, the phase arrangement is shown in Figs 2a and 2b. For the case of parallel arrangement (a), the uniform strain is assumed in the two phase, the upper bound is given by [16]

$$E_c = E_pV_p + E_mV_m \quad (10)$$

whereas in series arrangement of case (b) the stress assumed to be uniform in the two phases, the lower bound is

$$E_c = \frac{E_pE_m}{E_pV_m + E_mV_p} \quad (11)$$

Equivalent models for concrete systems were proposed by Hansen [3], and Kaplan [17].

For Equation 10 it is assumed that the Poisson ratios of constituent phases are equal. Whereas for Equation 11 ν_c will be given by

$$\nu_c = \frac{(\nu_pV_pE_m + \nu_mV_mE_p)}{(E_mV_p + E_pV_m)} \quad (12)$$

The bounds obtained from Equations 10 and 11 given in Fig. 3 as curves 1 and 2, respectively, are widely spaced and often unable to represent the experimental data. This implies that the assumption of either a state of uniform strain or uniform stress in the individual phases of the filled system is not sufficient to describe the modulus.

2.2.2. The Hashin and Shtrikman model

Improved bounds for the modulus of two-phase media were obtained by Hashin and Shtrikman who took into account the Poisson contraction of the constituent phases [14]. The overall response of the

composite was assumed to be isotropic and linearly elastic. The equations for the lower and upper bounds, respectively, are given in Equations 13 and 14

$$E_c = \frac{9\left(K_m + \frac{V_p}{[1/(K_p - K_m)] + [3V_m/(3K_m + 4G_m)]}\right)\left(G_m + \frac{V_p}{[1/(G_p - G_m)] + [6(K_m + 2G_m)V_m/5(3K_m + 4G_m)G_m]}\right)}{3\left(K_m + \frac{V_p}{[1/(K_p - K_m)] + [3V_m/(3K_m + 4G_m)]}\right) + \left(G_m + \frac{V_p}{[1/(G_p - G_m)] + [6(K_m + 2G_m)V_m/5(3K_m + 4G_m)G_m]}\right)} \quad (13)$$

$$E_c = \frac{9\left(K_p + \frac{V_m}{[1/(K_m - K_p)] + [3V_p/(3K_p + 4G_p)]}\right)\left(G_p + \frac{V_m}{[1/(G_m - G_p)] + [6(K_p + 2G_p)V_p/5(3K_p + 4G_p)G_p]}\right)}{3\left(K_p + \frac{V_m}{[1/(K_m - K_p)] + [3V_p/(3K_p + 4G_p)]}\right) + \left(G_p + \frac{V_m}{[1/(G_m - G_p)] + [6(K_p + 2G_p)V_p/5(3K_p + 4G_p)G_p]}\right)} \quad (14)$$

K and G are the bulk and shear moduli and m and p refer to matrix and particle, respectively. The Poisson ratio of the composite is given by

$$\nu_c = \frac{3K_c - 2G_c}{2(G_c + 3K_c)} \quad (15)$$

The separation of the Hashin upper and lower bound are dependent upon the modular ratio of particle to the matrix ($m = E_p/E_m$). When the moduli of the constituent phases are closely matched, the bounds predict values within 10%. In the case of a rigid polymeric-filled system where m is approximately 20 the bounds given by Equations 13 and 14, respectively, given as curves 3 and 4 in Fig. 4, are still widely spaced and therefore of limited predictive value. The Hashin–Shtrikman bounds (curves 3 and 4, Fig. 4), however, serve as a useful test of the approximate theories, since any solution outside these bounds must be regarded invalid.

2.2.3. The Hirsch model

Hirsch [18] proposed a relation for E_c, which is a summation of Equations 10 and 11

$$E_c = x(E_p V_p + E_m V_m) + (1 - x)\frac{E_p E_m}{(E_p V_m + E_m V_p)} \quad (16)$$

The model is illustrated in Fig. 2c. The parameters x and $1 - x$ are the relative proportions of material conforming to the upper and lower bound solutions, respectively; when $x = 0$ Equation 16 reduces to Equation 11 which can be identified with a poorly bonded filler. For the perfectly bonded filler, when $x = 1$ the equation reduces to Equation 10. This model was proposed for concrete systems to take into account the complex stress distribution in the individual phase. The empirical parameter x can be determined by curve fitting as illustrated in Fig. 3.

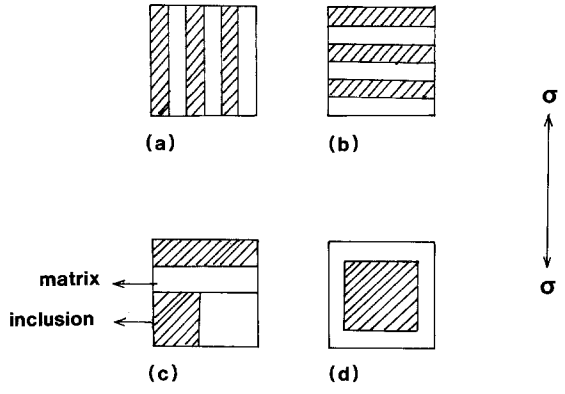

Figure 2 Models for particulate-filled composites. (a) Parallel (constant strain) model, (b) series (constant stress) model, (c) Hirsch's model, (d) Counto's model.

2.2.4. The Takayanagi model

Takayanagi *et al.* [19] combined Equations 10 and 11 and proposed a series–parallel model (Fig. 5)

$$E_c = \left(\frac{\alpha}{(1 - \beta)E_m + \beta E_p} + \frac{(1 - \alpha)}{E_p}\right)^{-1} \quad (17)$$

where parameters α and β represent the state of parallel and series coupling in the composite, respectively. Equation 17 was developed to predict the modulus of a crystalline polymer. The basic problem with the model is the determination of values for α and β.

Kraus and Rollmann [20] proposed an equivalent model for phase arrangements in a crystalline polymer. This model is particularly suitable for describing the performance of an interpenetrating network.

The arrangement of the series and parallel element is, however, an inherent difficulty with all the preceding models. There are also conceptual difficulties in relating these models to real systems.

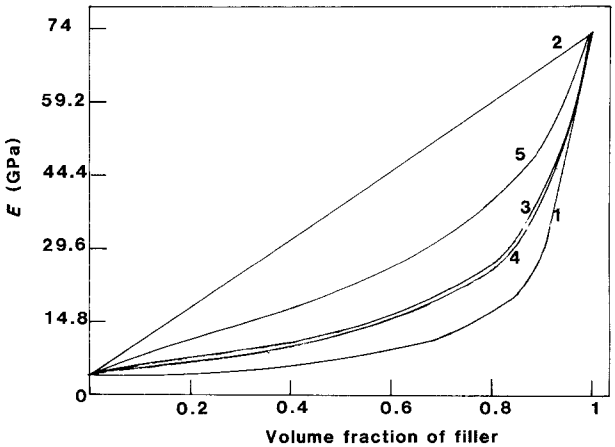

Figure 3 Relations between the modulus of filled resin and the volume fraction of filler for the simplified models shown in Fig. 2. Curves 1 and 2 are for the series and parallel model, respectively. Curves 3 and 5 are from the Hirsch model (Equation 16) by taking $x = 0.5$ and $x = 0.8$, respectively. Curve 4 shows the Counto model (Equation 18). All the curves were calculated using $E_m = 3.9$ GPa and $E_p = 72.4$ GPa.

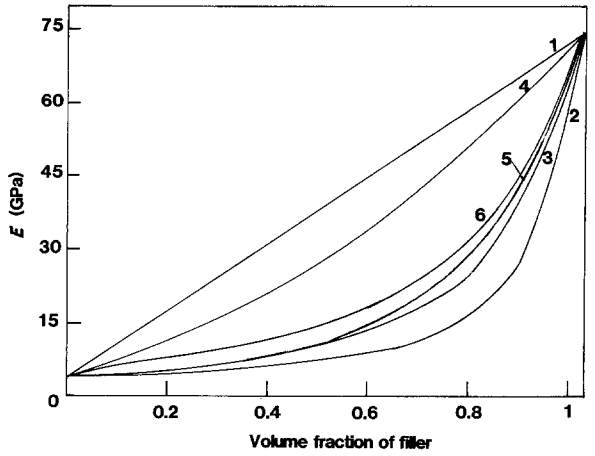

Figure 4 Theoretical prediction of the composite modulus. Curves 1 and 2 show the law of mixture lower and upper bound, respectively. Curves 3 and 4 show the Hashin lower and upper bound, respectively. Curves 5 and 6 are the approximate solution of the Ishai and Paul equations, respectively. All curves were calculated using E_m = 3.9 GPa and E_p = 72.4 GPa.

2.2.5. The Counto model

The simpler model, for a two-phase system proposed by Counto [21] assumes perfect bonding between the particle and the matrix. The modulus of the composite is given by

$$\frac{1}{E_c} = \frac{1 - V_p^{1/2}}{E_m} + \frac{1}{(1 - V_p^{1/2})/V_p^{1/2}E_m + E_p} \quad (18)$$

This model predicts moduli in good agreement with a wide range of experimental data, especially for concrete systems. It should be noted that when x takes a value of 0.5 in Equation 16 it coincides with the values predicted from Equation 18 (see Fig. 3).

2.2.6. The Paul model

For the approximate solution obtained by Paul [15], the constituents are assumed to be in a state of macroscopically homogeneous stress. Adhesion is assumed to be maintained at the interface of a cubic inclusion embedded in a cubic matrix. When a uniform stress is applied at the boundary the elastic modulus of the composite is given by

$$E_c = E_m\left(\frac{1 + (m - 1)V_p^{2/3}}{1 + (m - 1)(V_p^{2/3} - V_p)}\right) \quad (19)$$

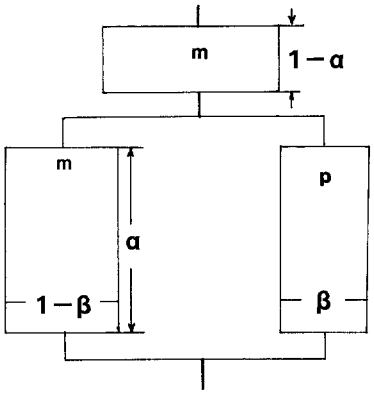

Figure 5 The Takayanagi model for a two-phase polymer system combining elements of parallel and series models (m refers to matrix, p to filler). β is a function of volume fraction of the parallel element and α of the series element.

Using the same model, for uniform displacement at the boundary Ishai and Cohen [22] obtained the following equation

$$E_c = E_m\left(1 + \frac{V_p}{m/(m - 1) - V_p^{1/3}}\right) \quad (20)$$

in which $m = E_p/E_m$.

2.2.7. The Chow model

For a system filled with non-spherical particles, the type and degree of orientation can completely modify the deformation behaviour. With oriented particles, the composite is anisotropic. Chow [23] included the anisotropy of the particles in the form of the aspect ratio p.

The longitudinal Young's modulus for an ellipsoidal particle embedded in the matrix with major axis aligned along the direction of applied stress is

$$E_c = E_m\left(1 + \frac{(K_p/K_m - 1)A_1 + 2(G_p/G_m - 1)B_1}{2B_1A_3 + A_1B_3}\right) \quad (21)$$

In which

$$A_i = 1 + (G_p/G_m - 1)(1 - V_p)\beta_i$$
$$B_i = 1 + (K_p/K_m - 1)(1 - V_p)\alpha_i \qquad i = 1, 3$$

where K and G are the bulk and the shear moduli, α_i and β_i are functions of aspect ratio p and Poisson's ratio of the matrix (see Appendix A for further details).

Equation 21 reduces to the Kerner equation for spherical particles (p = 1) and as $p \to \infty$ Equation 21 approaches the parallel model of the rule of mixtures.

2.2.8. The Cox model

For an aligned short fibre composite, Cox [24] assumed that the load was transferred to the fibre from the surrounding matrix by a shear mechanism. Any tensile stresses in the matrix were neglected. The longitudinal Young's modulus of the composite is given by

$$E_c = E_m(1 - V_f) + E_fV_f\left(1 - \frac{\tanh z}{z}\right) \quad (22)$$

where

$$z = \frac{l}{2r}\left(\frac{2G_m}{E_f \ln (R/r)}\right)^{1/2}$$

l is the length, r the radius and $2R$ the centre-to-centre distance of the fibres. The filler shape was characterized by the aspect ratio, $p = l/2r$, where $p \gg 1$. The elastic modulus of short aligned fibre composites can be predicted from the above equation. In a real composite system the fibres will usually be random, therefore an appropriate orientation factor would be needed for the application of Equation 22.

3. Limitations of the theoretical models

Having summarized the models available for the prediction of the moduli of a filled system, their applicability and limitations will be discussed. At this point it should be stressed that in the above survey no attempt has been made to discuss the approaches in

detail but to demonstrate the number of theoretical hypotheses available to describe the moduli of the filled system. For a discussion of the detailed theoretical base of each the reader is referred to Hashin [25] and Hill [26].

The lower and upper bound solutions given by Equations 10 and 11 assume that the individual phases are under uniform strain or stress, respectively. In practice, however, the filler particles may not be completely separated from one another and the reinforcement element may, on the microlevel, effectively be an aggregate of smaller particles. Thus in response to the applied load the stress will be distributed unevenly between the particles and aggregates and the assumption of either uniform stress or uniform strain is clearly an oversimplification. To account for the complex stress and phase distribution, Hirsch [18], Takayanagi [19], Kraus [20], and Wu [27] considered differing combinations of the upper and lower bounds of the laws of mixtures. All of these require an empirical factor which is determined by a curve fitting routine, to furnish a phenomenological description of the experimental data.

The theories which deal with filled systems indicate that the elastic modulus for a given particle and matrix depend only upon the volume fraction of filler and not the particle size, however, generally the modulus increases as the particle size decreases [9, 28–30]. Lewis and Nielsen [9] postulated that as the particle size decreases, the surface area increases providing a more efficient interfacial bond. This would also be accompanied by a tendency for increased agglomeration of the particles.

The properties of the composites may also be affected by changes in particle shape. Bueche [31] observed that different filler shapes resulted in differing mechanical properties. The effect was especially pronounced with larger or non-spherically shaped particles where a preferred orientation could modify the deformation behaviour. Wu [32] proved theoretically that disc-shaped particles gave better reinforcement than, needle or spherical shaped particles but ignored the anisotropy associated with non-spherical particles in the composite. Chow [23] has dealt with this problem for aligned ellipsoidal particles and predicted both longitudinal and transverse moduli. The effects of filler size and filler surface area were not taken into account, however, it is highly unlikely that in practice, the filler particles can be uniformly arranged in the manner assumed by Chow so that the experimental confirmation of both theories has yet to be established.

The particle size distribution affects the maximum packing fraction ϕ_m; mixtures of particles with differing size can pack more densely than monodispersed particles because the small ones can fill the interstitial space between the closely packed large particles to form an agglomerate. These aggregated particles may be able to carry a larger proportion of the load than the primary particles to yield a higher modulus, at the same volume fraction predicted by most theories. This effect is illustrated in Figs 6 and 7 where a differing reinforcing efficiency for glass beads compared to

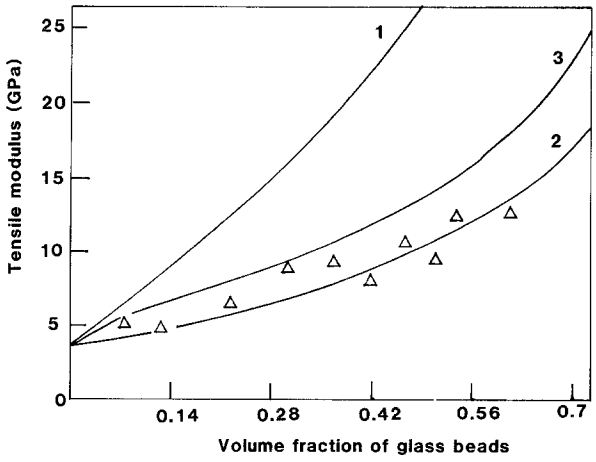

Figure 6 Comparison of theoretical and experimental moduli of graded glass bead composites taken from Ahmed and Jones [34]. Curves 1 and 2 show the Hashin upper and lower bounds, respectively and curve 3 the Paul approximation. All curves were calculated using $E_m = 3.9\,GPa$, $\nu_m = 0.39$, $E_p = 70\,GPa$ and $\nu_p = 0.22$.

irregularly shaped sand particles was observed by Ahmed and Jones [33, 34]. An empirical modification of the Kerner equation proposed by Lewis and Nielsen [9], introduced a curve fitting parameter ϕ_m. A similarly modified Kerner equation which also included a filler interaction factor was proposed by Dickie [35]. Each of these equations appears to satisfactorily describe the data of the individual authors. One should note the comment by Christensen [36] on the Kerner equation; that the explicit error in the Kerner equation cannot be "pinpointed because of the brevity of the derivation". This, therefore, casts doubt on the Kerner equation and its subsequent modifications. Recently McGee and McCullough [37] have formulated empirical rules for predicting the modulus of a filled system with a rigid or non-rigid matrix as the continuous phase. Their approach seems to be more reliable than the Kerner equation. A new approach to model the statistical distribution of the filler particles has recently been attempted by Guild and Young [38]. They applied the finite element technique to statisti-

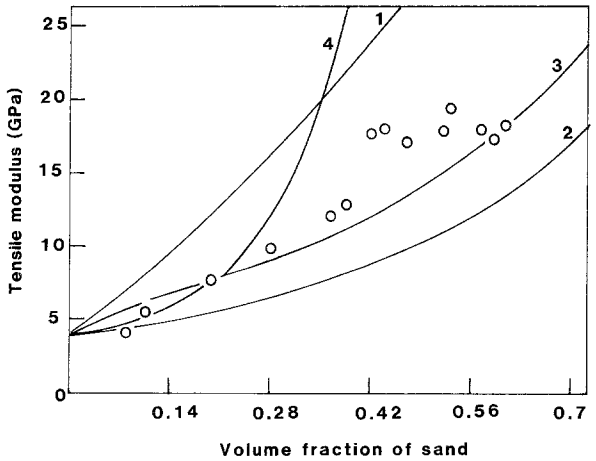

Figure 7 Comparison of theoretical and experimental data of Ahmed and Jones [33] for graded sand-filled polyester composite with the value of E, predicted by various models. Curves 1 and 2 show the Hashin upper and lower bounds, respectively and curve 3 the Paul approximation. Curve 4 shows the Mooney equation (Equation 3, $S = 1.35$ and $\nu_m = 0.39$). All curves were calculated using $E_m = 3.9\,GPa$ and $E_p = 72.4\,GPa$.

cally distributed filler particles in a two-phase system. They found a good correlation between the predicted and the experimentally observed moduli for their glass-epoxy filled composites. Its application to a wider range of experimental data is, however, required to establish its full potential.

Most of the theories which explain the reinforcing action of a filler assume perfect adhesion between the filler and the polymer matrix. The case of imperfect adhesion in the elastic case was, however, discussed theoretically by Sato and Furukawa [39]. They assumed that the non-bonded particles acted as holes and, therefore, predicted a decrease in modulus with increasing filler content. One can argue that the non-bonded particles do not act entirely as holes, since they also restrain the matrix from collapsing. In this case the modulus of the filled system should increase with increasing filler content, which is the general behaviour expected. A change of the matrix–filler adhesion has a smaller effect on modulus than on strength. The latter is much more dependent on surface pretreatment [28, 40, 41]. In fact, the degree of adhesion does not appear to be an important factor as long as the frictional forces between the phases are not exceeded by the applied stress. In most filled systems there is a mismatch in the coefficients of thermal expansion which is reflected as a mechanical bond resulting from thermally induced stresses. Brassell [42] found that the degree of bonding between the phases does not appear to have any influence on mechanical properties at liquid nitrogen temperature and this was attributed to the compressive stresses on the filler particle. In most cases even if the adhesion is poor, the theories are valid because there may not be any relative motion across the filler–matrix interface. Spanoudakis and Young [28] investigated glass filled epoxy resin and found that the best overall mechanical properties were obtained from composites containing particles treated with a coupling agent.

It is clear from the foregoing discussion that the modulus of a filled system is a detailed function of the microstructure as well as the explicit nature of the interfacial adhesion.

4. Comparison of experimental data with theory

The theoretical curves predicted by the various models are compared in Fig. 4. The curves were obtained for a typical particulate filled thermosetting resin composite; $E_p = 72.4\,\text{GPa}, \nu_p = 0.22, E_m = 3.9, \nu_m = 0.39$. The Hashin upper and lower bounds provided by Equations 13 and 14 (curves 3 and 4, respectively) are widely spaced and of limited predictive value, whereas the Paul estimation given by Equation 19 (curve 6) lies between the Hashin lower and upper bound, thus providing an intermediate solution. At low V_p, the Hashin lower bound coincides with the Ishai estimation (curve 5). Above $V_p = 0.5$ the Ishai estimation predicts higher values of modulus than the Hashin lower bound. The ability of the various theoretical models to describe experimental data is illustrated with reference to the data of Spanoudakis and Young [28].

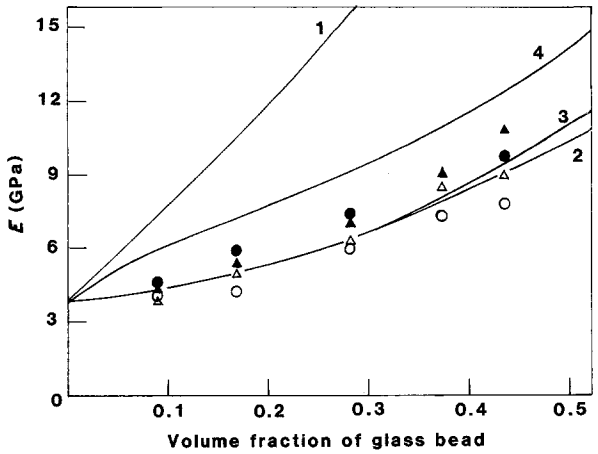

Figure 8 Comparison of theoretical and experimental data of Spanoudakis and Young [28] for glass-filled epoxy composite with the value of E, predicted by various models. Curves 1 and 2 are the Hashin upper and lower bounds, respectively. Curves 3 and 4 are the Ishai and Paul approximations, respectively. The predictions are based on the properties of the glass beads and the matrix, $E_m = 3.7\,\text{GPa}$, $\nu_m = 0.39$, $E_p = 70\,\text{GPa}$, $\nu_p = 0.22$. (▲, 62 μm treated, △, untreated; ●, 4.5 μm treated, ○, untreated).

In Fig. 8 the modulus of glass-filled epoxy composites are compared with various theoretical predictions. The Hashin upper bound (curve 1) grossly overestimates the data, whereas the Paul equation (curve 4) overestimates the results to a lesser extent. The data fall on the curve predicted by the Hashin lower bound (curve 2) and Ishai estimation (curve 3). Clearly, it is hard to choose between Hashin and Ishai solutions.

The appropriate theoretical solution is further complicated by the difficulty of incorporating the effect of particle size. It appears from the data in Fig. 8 that the larger particles are a more effective reinforcement, especially at higher volume fractions. Vollenberg and Heikens [30], however, observed that fine silica particles and chalk particles were more effective in the thermoplastic, polystyrene. They attempted to explain these results with the formation of a more dense matrix in the interfacial region. Moloney *et al.* [67] were, however, unable to observe a size effect for silica-filled epoxy resin. Similarly, Ahmed and Jones [34] were unable to observe differences between fine and coarse glass beads, in a thermosetting polyester resin. Their work did, however, demonstrate one of the deficiencies of these theories, namely the formation of agglomerates. As shown in Fig. 6, grading the spherical particles yielded only a slight improvement whereas as shown in Fig. 7 grading the angular particles gave a much bigger improvement to the modulus of the composite. Agglomeration is an important aspect of particulate reinforcement of elastomers. As discussed in Section 2.1 the Mooney equation gives a good prediction of this reinforcing effect and by use of a crowding factor is able to differentiate between different grades of carbon black. As seen in Fig. 7, the Mooney equation does not apply to filled rigid thermosetting resins. One of the reasons why a fully embracing theory has not been developed, can also be gained from the work on sand-filled resin [33] where it was shown that the thermal history had a strong influence on the modulus. This was attributed to the generation

of thermal compressive stresses associated with local variations in particle volume fraction which arises from the agglomeration of graded angular particles. Thus an appropriate theoretical prediction will have to include the statistics of particle coalescence and its effect on the thermomechanical properties of the composite. In addition to this the possible formation of an interphase, either as a result of conformational changes in a linear polymer or the presence of a coupling agent [68], makes it clear that the approximate solutions of Ishai [22] and Paul [15] still have much value. The development of a statistical model along the lines of Guild and Young [38] may prove more appropriate.

5. Strength of particulate composites

As pointed out by Nielsen [43], the theories for the strength of filled systems is less developed than that for the moduli. Except for the case of filled rubber, there are severe limitations to current thinking.

5.1. The Sahu–Broutman model

In the approach of Sahu and Broutman [44], they assumed that the composite fails when one element is fractured as a result of a stress concentration around the filler particle. It follows that the strength drops rapidly with the addition of small amounts of filler, and remains essentially at that level with further additions. With this assumption, they used a finite element analysis to model the composite and correlated the results with the experimental strengths of a glass sphere filled thermosetting resin. The theoretical predictions did not give a good fit to the experimental data because the model neglects particle interactions. In addition the composites may not have failed as a result of the failure of the first element.

5.2. The power law

The second approach assumes that the strength of a particulate composite is determined by the effective available area of load bearing matrix due to the presence of the filler [45–49].

In the case of a poor bond between the matrix and the filler (i.e., no stress transfer), and the absence of a stress concentration at the particle–matrix interface, the strength is described by a power law

$$\sigma_{cu} = \sigma_{mu}(1 - aV_p^n) \quad (23)$$

where σ_{cu} and σ_{mu} are the ultimate tensile strengths of the composite and the matrix, respectively, V_p the volume fraction of the filler and a and n constants depending on the assumed particle shape and arrangement in the model composite.

Nielsen [45] has introduced a stress concentration factor, K with a suggested value of 0.5. For cubic particles embedded in a cubic matrix Equation 23 can be written as

$$\sigma_{cu} = \sigma_{mu}(1 - V_p^{2/3})K \quad (24)$$

Nicolais and Narkis [48], considered a cubic matrix filled with uniformly dispersed spherical particles, where fracture was assumed to occur in the minimum cross-section of the continuous phase which was perpendicular to the applied load. Equation 23 becomes

$$\sigma_{cu} = \sigma_{mu}(1 - 1.21V_p^{2/3}) \quad (25)$$

Piggott and Leidner [50] argued that the uniform filler arrangement assumed in most models was unlikely in practice and proposed an empirical relationship

$$\sigma_{cu} = K\sigma_{mu} - bV_p \quad (26)$$

where K is a stress concentration factor and b a constant dependent upon the particle–matrix adhesion.

Landon *et al.* [51] proposed a similar equation

$$\sigma_{cu} = \sigma_{mu}(1 - V_p) - k(V_p)d \quad (27)$$

where d is the average particle diameter and k the slope of the plot of tensile strength against mean particle diameter.

5.3. The Leidner–Woodhams equation

A simpler but more elaborate approach has been developed by Leidner *et al.* [52]. The model composite consisted of spherical particles embedded in an elastic matrix. In order to apply reinforcement theory [53] the particle size was approximated to a cylinder. In this way the stress distribution in the bead, at the breaking point could be determined. In the case of non-bonded particles, the stress transfer between the particle and the matrix was assumed to occur as a result of the combination of particle–matrix friction and residual compressive stresses which act upon the particle–matrix interface. In the case of well bonded particles the stress is transferred through shear mechanism. The maximum stress in the particle is, therefore, dependent upon the shear strength of the matrix and on the strength of particle–matrix bond. The ultimate tensile strength of the composite was taken simply as the sum of the maximum load carried by the matrix and the filler and given by

$$\sigma_{cu} = (\sigma_a + 0.83\tau_m) + \sigma_a K(1 - V_p) \quad (28)$$

for good interfacial adhesion and

$$\sigma_{cu} = 0.83\sigma_{th}\alpha V_p + k\sigma_{mu}(1 - V_p) \quad (29)$$

in the case of no interfacial adhesion. σ_a and σ_{mu} are the strength of the interfacial bond and the ultimate strength of the matrix, respectively, τ_m the shear strength of the matrix, K the stress concentration factor, k a parameter which depends on the particle size, σ_{th} the thermal compressive stress acting on the boundary of the particle and α the coefficient of friction.

There have been a number of attempts to correlate the strength of particulate-filled systems with the diameter of the particle, d. For example Hojo *et al.* [54, 55] have found that the strength of silica-filled epoxy decreases as the size of the particles increase following a relationship of the form

$$\sigma_{cu} = \sigma_{mu} + kd^{-1/2} \quad (30)$$

where k is a constant and d is the mean particle diameter.

6. Limitations of the theoretical models

Particle size can greatly affect the tensile strength of

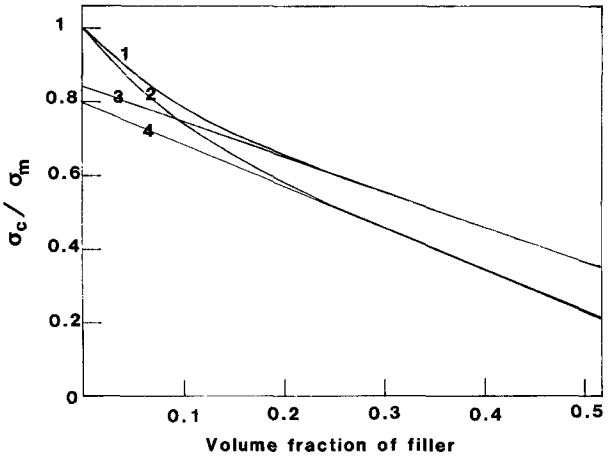

Figure 9 Comparison of strength predicted from linear and power laws. Curve 1 shows the Neilsen equation with $K = 1$ (Equation 24). Curve 2 is from the Nicolais and Narkis equation (Equation 25). Curves 3 and 4 are for the Piggott equation (Equation 26) with $K = 0.84, b = 1$ and $K = 0.8, b = 1.2$, respectively. The value of K has been chosen to fit the linear portions of curves 1 and 2.

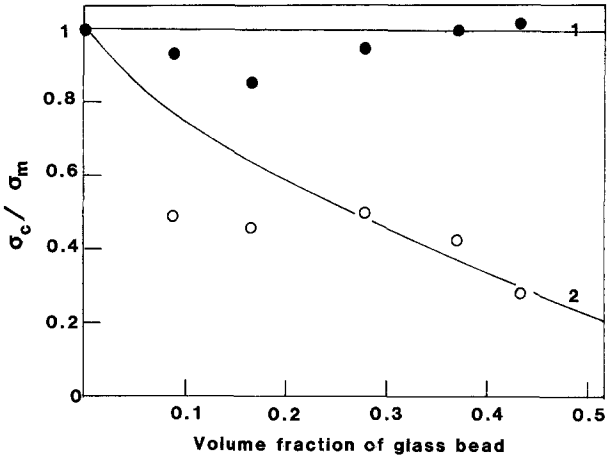

Figure 10 Comparison of the ratio of composite fracture strength to matrix strength, as a function of V_p. The upper bound (curve 1) is for $\sigma_c = \sigma_m$ and the lower bound (curve 2) Nicolais and Narkis equation (Equation 25). The experimental data is for glass–epoxy filled composite [28]. (●, 4.5 μm diameter particles with surface pretreatment, ○ untreated).

filled systems [49, 51, 52]. In general, the tensile strength increases with a decrease in particle size. The increase in interfacial area which provides a more effective interfacial bond is considered to be the most important factor. Particle size is also related to the flaw size dependence of the material. Goodier [56] has shown that the stress field near a particle is independent of the particle size. The volume of polymer that experiences a given stress concentration is, however, increased with increase in particle size; therefore the probability of finding a large flaw increases with increased particle size.

The effect of interfacial adhesion on the strength can be rationalized in a similar fashion since a poor particle–matrix bond will act as an inherent flaw with the production of a cavity equal to its size.

The shape of the inclusion is expected to play an important role in determining the strength of the filled system. Since, with a non-regularly shaped inclusion, the weakening is due to a high stress concentration coupled with a size effect, and with rounded cracks and inclusions the stress concentration is much less severe than for inclusions with sharp corners.

The foregoing discussion clearly demonstrates that the models available for predicting strength would set an upper limit on the strength of the filled system. When predicting the strength of filled material by employing the power law, the choice of appropriate constants is governed by the particle shape and arrangement in the geometric model, in addition the stress concentration will lower these values by an undetermined amount.

On the other hand, in the Leidner and Woodhams analysis, the thermal stresses (σ_{th}) and particle–matrix bond strength (σ_a) are difficult to measure for real composites. At very low V_p, estimates of the thermal stresses can be made [57], but at high V_p the calculations are complicated by the presence of neighbouring particles. Also, in real situations the filler particles rarely have uniform diameters presenting difficulties with the correct choice of values for use in Equations 27, 29 and 30, therefore, these equations are of limited value.

7. Comparison of experimental data with theory

In Fig. 9, the strength predictions from the various theoretical approaches as a function of V_p are compared. It can be seen that Equation 26 (curves 3 and 4) almost predicts identical values to a power law expression (curves 1 and 2), at volume fraction greater than 0.2. Linear equations such as Equations 26 and 27 are ineffective in describing the data at low V_p, however, they may be considered as useful empirical equations for the use at intermediate to high volume fraction of filler.

In Fig. 10, the relative strength of glass beads filled epoxy composite [28] is compared with Equation 25. The correlation is not so good because of the uncertainties which may arise as a result of the stress concentration enhanced by poor particle–matrix adhesion, which cannot be quantified experimentally and is difficult to model theoretically. An alternative system would be a fracture mechanics approach. This has been reviewed elsewhere [58].

Although the addition of rigid brittle particles to a polymer matrix tends to cause a reduction in strength of the filled material, it is well established that crack propagation becomes more difficult in such materials [58]. Several possible mechanisms can be used to explain this phenomena. Firstly, the toughness may be increased by the filler particles diverting the crack and increasing the fracture surface area, however, the increase in fracture surface area is insufficient to account for the large rise in toughness. Secondly, in the case of some filled systems containing for example, metallic or rubber particles [59], the energy may be absorbed by the deformation of the filler. This is most unlikely with brittle particles. Thirdly, the increase in toughness may arise from the increased plastic deformation of the matrix. Fourthly, the toughening may occur by obstacle pinning of the crack causing the crack front to bow out between the particles.

Lange and Radford [60] have discussed the above mechanisms. They suggested that the most likely mechanism is the interaction of a crack front with the

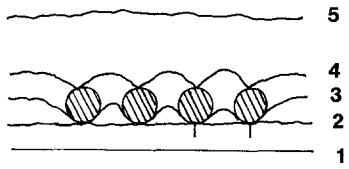

Figure 11 Various stages of crack-pinning mechanism in a rigid particulate-filled composite. 1. Approach, 2. Interaction and pinning, 3. Bow-out, 4. Coalescence, 5. Breakaway [58].

dispersed phase, as illustrated in Fig. 11. During fracture, a moving crack front is momentarily pinned at a position of inhomogeneity within the matrix. This interaction leads to a bowing out of the crack front from the pinned positions, thus increasing its total length. On breaking away from the pinned position, the crack front creates characteristic steps on the fracture surface. These steps are formed by overlapping crack fronts as it bows out between the dispersed particles.

On investigation of the effect of particle size on the fracture surface energy, Lange and Radford [69], Mallick and Broutman [61] and Broutman and Sahu [62] found an increase in fracture surface energy with increasing volume fraction up to a maximum at around 0.2. Above 0.2 the fracture surface energies decreased becoming independent of particle diameter for glass sphere filled brittle polymeric composites. These results were explained by assuming that the effectiveness of pinning is a function of overlapping stresses associated with the crack front as it moves between the dispersed particles.

Fractographic studies have provided strong evidence for the crack pinning mechanism in particulate reinforced thermosetting polymers. Maxwell *et al.* [63] pointed out that several factors impair the efficiency of the cracking pinning mechanism such as, crack tip blunting through localized shear yielding, and a poor particle–matrix adhesion. For the latter, Spanoudakis and Young [28, 64] showed that for a glass–epoxy system, the crack propagation path is strongly affected by the improvement in particle–matrix adhesion. With untreated particles the cracks propagated around the equator, but with particles treated with a coupling agent, the crack propagated through the matrix above or below the poles of the particles. They observed the highest fracture toughness for composites in which poor particle–matrix interfacial adhesion existed. They postulated that debonding helped crack initiation but hindered crack propagation since crack bifurcation and branching took place. The highest level of toughness was achieved with the introduction of rubber particles in particulate-filled polymer where simultaneous crack pinning and localized plastic deformation occurred [65].

8. Conclusions

The state of the interface between the particles and matrix, the distribution, size and shape of the filler particles, affect the macroscopic behaviour of particulate filled composites, but they have not been satisfactorily modelled, theoretically. The variety of sources of experimental data rule out a preferred model for the prediction of macroscopic behaviour. Since individual models have been developed to describe a particular set of experimental data, a fresh theoretical approach together with systematic experimental studies is required.

Acknowledgement

The authors wish to thank the Government of Pakistan for the financial support to SA.

Appendix A. The Chow equation

For ellipsoid particles oriented along their major axis, the tensile modulus is given by

$$E_c = E_m\left(1 + \frac{(K_p/K_m - 1)A_1 + 2(G_p/G_m^{-1})B_1}{2A_3B_1 + A_1B_3}\right) \quad \text{(A1)}$$

where K and G are bulk modulus and shear modulus.

$$B_i = 1 + (K_p/K_m - 1)(1 - V_p)\alpha_i \quad \text{(A2)}$$

$$A_i = 1 + (G_p/G_m - 1)(1 - V_p)\beta_i \quad i = 1, 3 \quad \text{(A3)}$$

The parameters α and β are given by

$$\alpha_1 = 4\pi Q/3 - 2(2\pi - I)R \quad \text{(A4)}$$

$$\alpha_3 = 4\pi Q/3 - 4(I - \pi)R \quad \text{(A5)}$$

$$\beta_1 = \left(\frac{4\pi}{3} - \frac{4\pi - 3I}{1 - p^2}\right)Q - 4(I - 2\pi)R \quad \text{(A6)}$$

in which p = axial ratio (c/a)

$$\beta_2 = \left(\frac{4\pi}{3} - \frac{(4\pi - 3I)p^2}{1 - p^2}\right)Q + (4\pi - I)R \quad \text{(A7)}$$

where

$$Q = \frac{3}{8\pi}\left(\frac{1}{1 - \nu_m}\right) \quad \text{and} \quad R = \frac{1}{8\pi}\left(\frac{1 - 2\nu_m}{1 - \nu_m}\right) \quad \text{(A8)}$$

ν_m is the Poisson's ratio of the matrix. For $p < 1$

$$I = \frac{2\pi p}{(1 - p^2)^{3/2}}[\cos^{-1}p - p(1 - p^2)^{1/2}] \quad \text{(A9)}$$

and for $p > 1$

$$I = \frac{2\pi p}{(p^2 - 1)^{3/2}}[p(p^2 - 1)^{1/2} - \cosh^{-1}p] \quad \text{(A10)}$$

When $p \to 1$

$$I = 4\pi/3 \quad \text{(A11)}$$

$$\alpha_1 = \alpha_3 = \alpha = \frac{1}{3} - \left(\frac{1 + \nu_m}{1 - \nu_m}\right) \quad \text{(A12)}$$

$$\beta_1 = \beta_3 = \beta = \frac{2}{15}\left(\frac{4 - 5\nu_m}{1 - \nu_m}\right) \quad \text{(A13)}$$

References

1. A. EINSTEIN, in "Investigation on Theory of Brownian Motion" (Dover, New York, 1956) (English translation).
2. H. M. SMALLWOOD, *J. Appl. Phys.* **15** (1944) 758.
3. T. C. HANSEN, *J. Amer. Conc. Inst.* **62** (1965) 193.
4. Z. HASHIN, *Bull. Res. Coun. Israel* **5C** (1955) 46.
5. M. MOONEY, *J. Colloid Sci.* **6** (1951) 162.
6. J. G. BRODNYAN, *Trans. Soc. Rheology* **3** (1959) 61.
7. E. GUTH, *J. Appl. Phys.* **16** (1951) 21.

8. E. H. KERNER, *Proc. Phys. Soc.* **69B** (1956) 808.
9. T. LEWIS and L. NIELSEN, *J. Appl. Polym. Sci.* **14** (1970) 1449.
10. J. E. ASHTON, J. C. HALPIN and P. H. PETIT, "Primer on Composite Analysis" (Technomic, Stamford, CN, 1969).
11. K. D. ZIEGEL and A. ROMANOV, *J. Appl. Polym. Sci.* **17** (1973) 1119.
12. L. E. NIELSEN, *J. Appl. Phys.* **4** (1970) 4626.
13. R. HILL, *J. Mech. Phys. Solid* **11** (1963) 357.
14. Z. HASHIN and S. SHTRIKMAN, *J. Mech. Phys. Solid* **11** (1963) 127.
15. B. PAUL, *Trans. Amer. Inst. Mech. Eng.* **36** (1960) 218.
16. L. J. BROUTMAN and R. H. KROCK, "Modern Composite Materials" (Addison Wesley, Reading, Massachusetts, 1967).
17. M. F. KAPLAN, *RILEM Bull.* **1** (1959) 58.
18. T. J. HIRSCH, *J. Amer. Conc. Inst.* **59** (1962) 427.
19. M. TAKAYANAGI, S. NEMURA and S. MINAMI, *J. Polym. Sci.* **5C** (1964) 113.
20. G. KRAUS and K. W. ROLLMANN, in "Multi Component System", edited by F. Gould (American Chemical Society, New York, 1971), Chap. 12, p. 189.
21. U. J. COUNTO, *Mag. Concr. Res.* **16** (1964) 129.
22. O. ISHAI and L. J. COHEN, *Int. J. Mech. Sci.* **9** (1967) 539.
23. T. S. CHOW, *J. Polym. Sci. Polym. Phys.* **16** (1978) 959.
24. H. L. COX, *Brit. J. Appl. Phys.* **3** (1952) 72.
25. Z. HASHIN, *Appl. Mech. Rev.* **17** (1964) 1.
26. R. HILL, *J. Mech. Phys. Solid* **11** (1963) 357.
27. T. T. WU, *J. Appl. Mech.* **32E** (1965) 211.
28. J. SPANOUDAKIS and R. J. YOUNG, *J. Mater. Sci.* **19** (1984) 487.
29. R. J. YOUNG, Proceedings of the International Conference, "Fillers '86" (PRI, London, 1986) Paper 13.
30. P. H. Th. VOLLENBERG and D. HEIKENS, *ibid.* (PRI, London, 1986) Paper 14.
31. A. M. BUECHE, *J. Polym. Sci.* **25** (1957) 139.
32. T. T. WU, *Int. J. Solids Struc.* **2** (1966) 1.
33. S. AHMED and F. R. JONES, *Composites* **19** (1988) 277.
34. *Idem, ibid.* **21** (1990) 81.
35. R. A. DICKIE, *J. Appl. Polym. Sci.* **17** (1973) 454.
36. R. M. CHRISTENSEN, "Mechanics of Composite Materials" (Wiley, New York, 1979).
37. S. McGEE and R. L. McCULLOUGH, *Polym. Composites* **2** (1981) 149.
38. F. J. GUILD and R. J. YOUNG, *J. Mater. Sci.* **24** (1989) 298.
39. Y. SATO and J. FURUKAWA, *Rubber Chem. Technol.* **36** (1963) 1081.
40. A. C. MOLONEY, H. H. KAUSH and H. R. STIEGER, *J. Mater. Sci.* **18** (1983) 208.
41. *Idem, ibid.* **19** (1984) 1125.
42. G. W. BRASSELL and K. B. WISCHMANN, *J. Mater. Sci.* **9** (1974) 307.
43. L. E. NIELSEN, *J. Compos. Mater.* **1** (1967) 100.
44. S. SAHU and L. J. BROUTMAN, *Polym. Eng. Sci.* **12** (1972) 9141.
45. L. E. NIELSEN, *J. Appl. Polym. Sci.* **10** (1966) 97.
46. L. NICOLAIS, E. DRIOLI and R. F. LANDEL, *Polymer* **14** (1973) 21.
47. L. NICOLAIS, *Polym. Eng. Sci.* **15** (1975) 137.
48. L. NICOLAIS and M. NARKIS, *ibid.* **11** (1971) 194.
49. L. NICOLAIS and L. NICODEMO, *ibid.* **13** (1973) 469.
50. M. R. PIGGOTT and J. LEIDNER, *J. Appl. Polym. Sci.* **18** (1974) 1619.
51. G. LANDON, G. LEWIS and G. BODEN, *J. Mater. Sci.* **12** (1977) 1605.
52. J. LEIDNER and R. T. WOODHAMS, *J. Appl. Polym. Sci.* **18** (1974) 1639.
53. A. KELLY, "Strong Solids" (Clarendon, Oxford, 1966) p. 161.
54. H. HOJO and W. TOYOSHIMA, 31st ANTEC, SPE Montreal, Canada (1973) (Technomic, 1973) p. 163.
55. H. HOJO, W. TANURA and N. KAWANURA, *Polym. Eng..Sci.* **14** (1974) 604.
56. J. N. GOODIER, *J. Appl. Mech. Trans. AME* **A3** (1933) 55.
57. J. SELLING, *J. Amer. Ceram. Soc.* **44** (1961) 419.
58. A. J. KINLOCH and R. J. YOUNG, "Fracture Behaviour of Polymers" (Applied Science, London, 1983) Chap. 11.
59. S. KUNZ-DOUGLASS, P. W. R. BEAUMONT and M. F. ASHBY, *J. Mater. Sci.* **15** (1980) 1109.
60. F. F. LANGE and K. C. RADFORD, *ibid.* **6** (1971) 1197.
61. P. K. MALLICK and L. J. BROUTMAN, *Mater. Sci. Engng* **8** (1971) 98.
62. L. J. BROUTMAN and S. SAHU, *ibid.* **8** (1971) 98.
63. D. L. MAXWELL, R. J. YOUNG and A. J. KINLOCH, *J. Mater. Sci. Lett.* **3** (1984) 9.
64. J. SPANOUDAKIS and R. J. YOUNG, *J. Mater. Sci.* **19** (1984) 473.
65. A. J. KINLOCH, D. L. MAXWELL and R. J. YOUNG, *ibid.* **20** (1985) 4169.
66. S. MALL, G. M. NEWAZ and M. FARHADINIA, *J. Rein. Plas. Compos.* **6** (1987) 138.
67. A. C. MOLONEY, H. H. KAUSH and H. R. STIEGER, Proceedings of the International Conference, "Fillers '86" (PRI, London, 1986) Paper 17.
68. F. R. JONES, in "Interfacial Phenomena in Composite Materials", edited by F. R. Jones (Butterworths, Guildford, 1989) pp. 6–7.

Received 13 February
and accepted 26 February 1990